

Coronavirus Disease (COVID-19): Spectrum of CT Findings and Temporal Progression of the Disease

Mingzhi Li, MD¹, Pinggui Lei, MD¹, Bingliang Zeng, MD¹, Zongliang Li, MD, Peng Yu, MD, Bing Fan, MD, Chuanhong Wang, MD, Zicong Li, MD, Jian Zhou, MD, Shaobo Hu, MD, Hao Liu, PhD

Coronavirus disease is an emerging infection caused by a novel coronavirus that is moving rapidly. High resolution computed tomography (CT) allows objective evaluation of the lung lesions, thus enabling us to better understand the pathogenesis of the disease. With serial CT examinations, the occurrence, development, and prognosis of the disease can be better understood. The imaging can be sorted into four phases: early phase, progressive phase, severe phase, and dissipative phase. The CT appearance of each phase and temporal progression of the imaging findings are demonstrated.

Keywords: COVID-19; 2019-nCoV; Coronavirus; Pneumonia; Tomography; X-ray computed.

© 2020 The Association of University Radiologists. Published by Elsevier Inc. All rights reserved.

INTRODUCTION

Coronavirus disease (COVID-19) is an emerging infection that is caused by a novel coronavirus (1–3). Since December 2019, when a number of COVID-19 cases emerged in Wuhan, Hubei Province, China, infection with COVID-19 has been declared an epidemic, with new cases emerging rapidly in other regions of China and across the world (4,5). By March 4, 2020, a total of 80,424 patients have been diagnosed with COVID-19 infection, and 2984 patients have died.

Chest imaging is of great importance for the diagnosis and management of patients with COVID-19 infection. However, it is easy to miss the diagnosis of early ground glass opacity (GGO) with plain chest radiography. Thus, computed tomography (CT), especially high-resolution CT (HRCT), is used for the early diagnosis of COVID-19 disease infection (6–9). High-resolution CT allows objective evaluation of the lung lesions, thus enabling us to better understand the pathogenesis of the disease. With serial CT examinations, the occurrence, development, and prognosis of the disease can be comprehensively

understood. Due to the high infectivity of the disease, histopathological examination has been limited. The advantage of CT over histologic examination is that CT can evaluate the whole lungs whereas histology is subject to sampling error, as it looks at only localized regions of the lungs. Here, we report the imaging findings and temporal progression of this disease.

METHODS AND MATERIALS

The cases reported in this study came from three hospitals (***) in China. All cases were confirmed by real-time reverse-transcriptase-polymerase chain reaction. Written informed consent was waived by our institutional review board. Due to the need for prevention and control of infection, chest radiography was adopted for ICU patients, whereas serial CT examinations were used for all other patients to monitor the dynamic changes of the disease.

CT examinations were performed with either a GE Optima 660 or Philips Brilliance CT scanner. The patients were placed in a supine position, with the head advanced and breathing on hold for scanning. The scanning parameters were as follows: 120 kV; 100–250 mAs; collimation of 5 mm; pitch of 1–1.5; matrix, 512 × 512. No contrast was administered. All images were transmitted to the postprocessing workstation to be reconstructed by high-resolution algorithms and conventional algorithms.

CLINICAL MANIFESTATIONS

The patients could be clinically divided into mild, moderate, severe, and critical according to the different clinical and radiological manifestations (10). The description for each

Acad Radiol 2020; ■:1–6

From the Radiology Department, Jiangxi Provincial People's Hospital, Nanchang 330006, China (M.L., B.Z., B.F., C.W., Z.L., J.Z., S.H.); Department of Radiology, The Affiliated Hospital of Guizhou Medical University, Guiyang, China (P.L.); Department of Radiology, Nanfeng County People's Hospital, Fuzhou, China (Z.L.); Radiology Department, Jinxian County People's Hospital, Nanchang, China (P.Y.); Medical AI (H.L.). Received February 28, 2020; revised March 5, 2020; accepted March 5, 2020. **Address correspondence to:** B. F. e-mail: 26171381@qq.com

¹ The authors contributed equally to the preparation of the manuscript.

© 2020 The Association of University Radiologists. Published by Elsevier Inc. All rights reserved.

<https://doi.org/10.1016/j.acra.2020.03.003>

type is as follows: Mild, patients whose clinical manifestations were minimal, and no pneumonia was seen on imaging; Moderate, patients who had clinical symptoms such as fever and respiratory symptoms, and manifestations of pneumonia were seen on imaging; Severe, patients with one or more of the following conditions: (1) shortness of breath with a respiratory rate ≥ 30 times/minute; (2) finger oxygen saturation $\leq 93\%$ in the resting state; (3) arterial partial pressure of oxygen/fraction of inspiration of oxygen ≤ 300 mmHg; and (4) lesion progression of more than 50% in 24–48 hours on the chest imaging. Critical: patients who met one or more of the following conditions: (1) respiratory failure requiring mechanical ventilation; (2) shock; and (3) failure of other organs, and the need for treatment in an intensive care unit.

RADIOLOGICAL MANIFESTATIONS

Imaging findings were sorted into four phases: early phase, progressive phase, severe phase, and dissipative phase (11). In the early phase, the patients demonstrated moderate clinical manifestations, where lesions were limited to single (Fig 1) or multiple (Fig 2) areas; and were distributed along the subpleural areas (Fig 3) or bronchi (12,13) (Fig 4). These findings indicated the characteristics of the spread of the lesions along the airway, starting with invasion of the bronchioles and alveolar epithelium of the cortical lung tissues, and extending gradually from the periphery to the center. The shapes of the lesions were nodular or patchy GGOs, with the blood vessels seen thickening and passing through the GGO. This was accompanied by the thickening of interlobular and intralobular septa, and the appearance of halo signs around the nodules (14,15) (Fig 5). The pathological basis may be congestion of alveolar septal capillaries, exudation of fluid into the alveoli and interstitial edema of the interlobular septum.

In the progressive phase, most of the COVID-19 lesions progressed rapidly, and corresponded to the severe type clinical classification. Compared to the early stage, the number of lesions increased significantly, with the

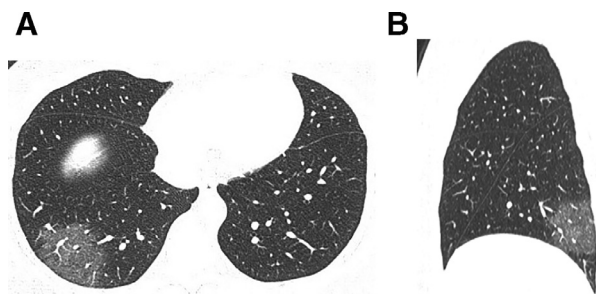


Fig. 1. A 40-year-old female patient with Coronavirus disease (COVID-19) pneumonia. (A) High-resolution CT scan obtained on day 3 from the onset of symptoms shows single ground glass opacities (GGO) in the posterior basal segment of the right lower lobe, within which thickened blood vessel shadows can be observed. (B) The sagittal reconstruction shows that the lesions are located in the posterior basal segment of the right lower lobe, with a pattern of subpleural distribution.

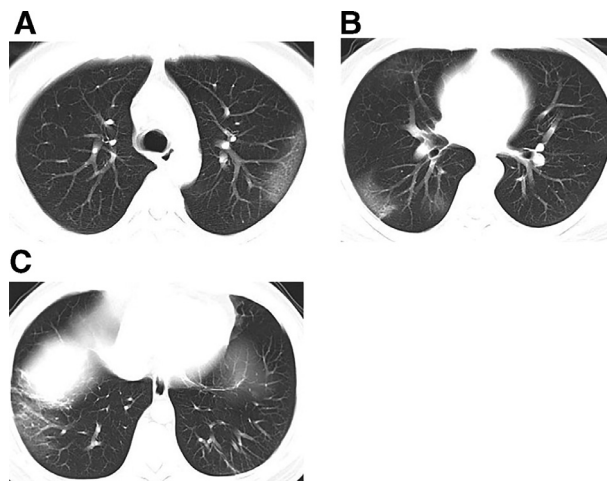


Fig. 2. A 37-year-old male patient with Coronavirus disease (COVID-19) pneumonia. (A–C) Multiple patchy ground glass opacities seen in both lungs, and the lesions show subpleural distribution, inside which the thickened vascular shadows are visible.

extent and density of the lesions increasing concurrently (16,17) (Fig. 6). The GGOs and the consolidations coexisted, showing both newly formed lesions and original

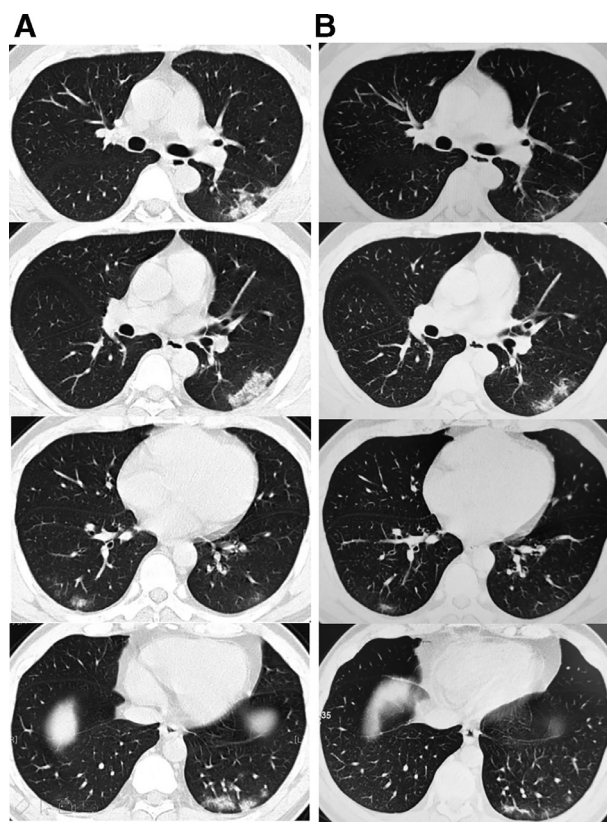


Fig. 3. A 40-year-old male patient with Coronavirus disease (COVID-19) pneumonia. (A) High-resolution CT scans obtained on day 5 from onset of symptoms show multiple consolidations in the two lungs with ground glass opacities, which are distributed peripherally in both lungs. (B) Follow-up high-resolution CT scans obtained on day 14 show a reduction of the lesions in both lungs after absorption, leaving fibrous cord-like shadows.

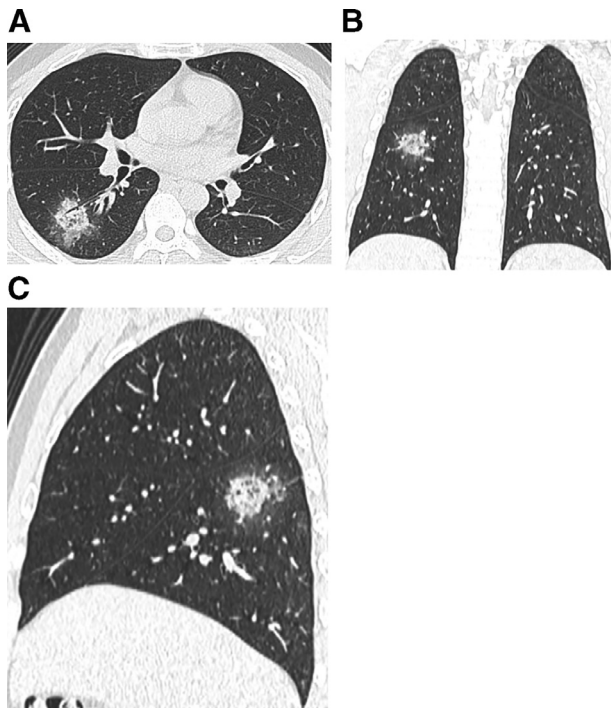


Fig. 4. A 31-year-old male patient with Coronavirus disease (COVID-19) pneumonia. (A) Nodular consolidations and GGO found in the dorsal segment of the right lower lobe, and the lesions distributed along the bronchial bundle, with the thickening of the interlobular septum and intralobular septum, and halo signs seen around the nodules. (B) Coronal reconstruction. (C) Sagittal reconstruction.

lesions with partial absorption (Fig 7). The mechanism of this pathology could be as follows: a large amount of cellular exudate accumulated in the alveolar cavity, causing interstitial

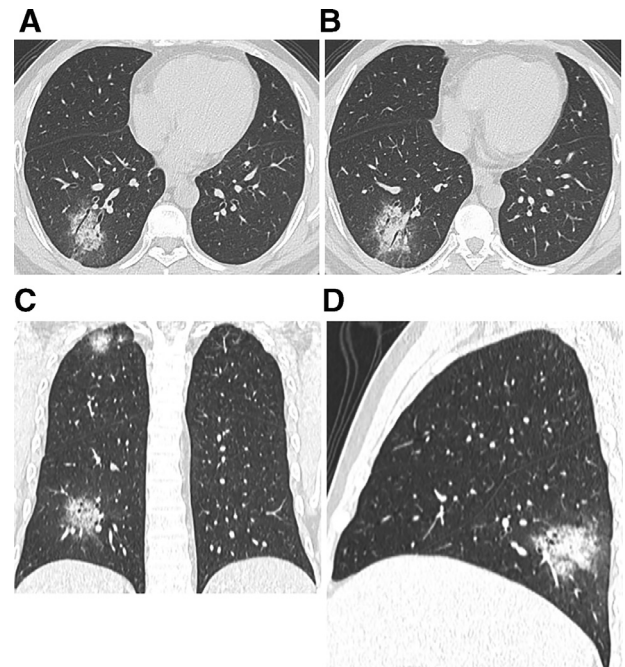


Fig 5. A 34-year-old male patient with Coronavirus disease (COVID-19) pneumonia, who is the older brother of the previous patient (Fig 4). (A–B) Patchy high-density shadows along the bronchial bundle in the posterior basal segment of the right lower lobe, around which halo signs can be seen, and air bronchogram can be seen inside the lesions. (C) Coronal reconstruction, from which lesions can also be seen in the apical segment of the right upper lobe. (D) Sagittal reconstruction.

vasodilation and exudation, and fusion of alveoli. The “crazy paving appearance” was apparent, suggesting the thickened interlobular and intralobular septae, and reflecting interstitial

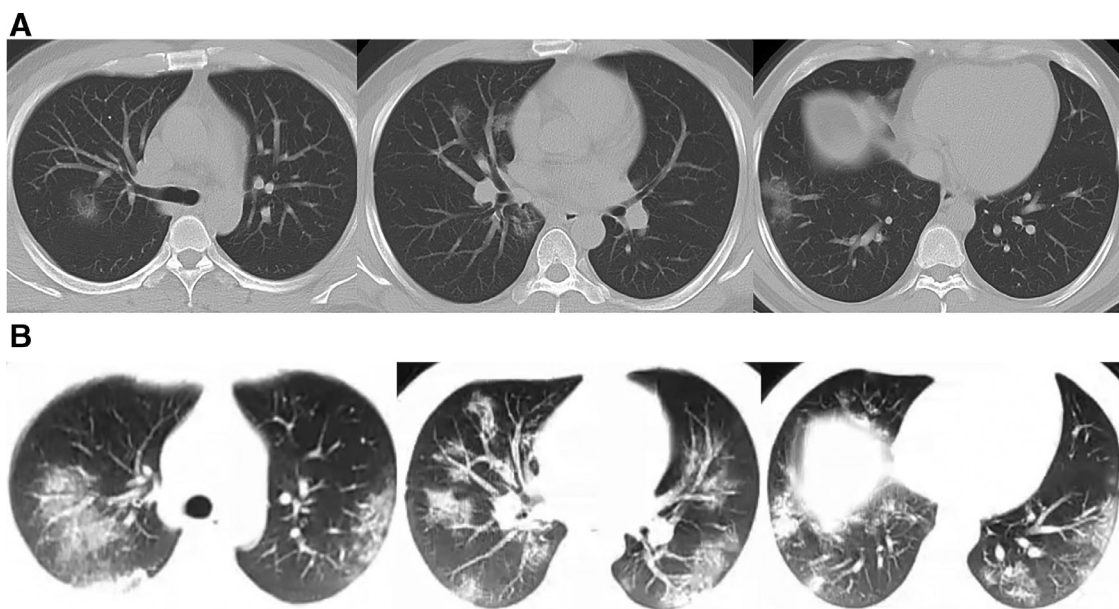


Fig. 6. A 35-year-old male patient with Coronavirus disease (COVID-19) pneumonia. (A) High-resolution CT scans obtained on day 3 from onset of the disease show multiple patchy consolidations and nodular ground-glass opacities, which are mainly distributed along bronchial bundles and subpleural regions. (B) CT images obtained on day 6 from onset of the disease show the progression of the disease, with elevated number, range and densities of the lesions in both lungs.

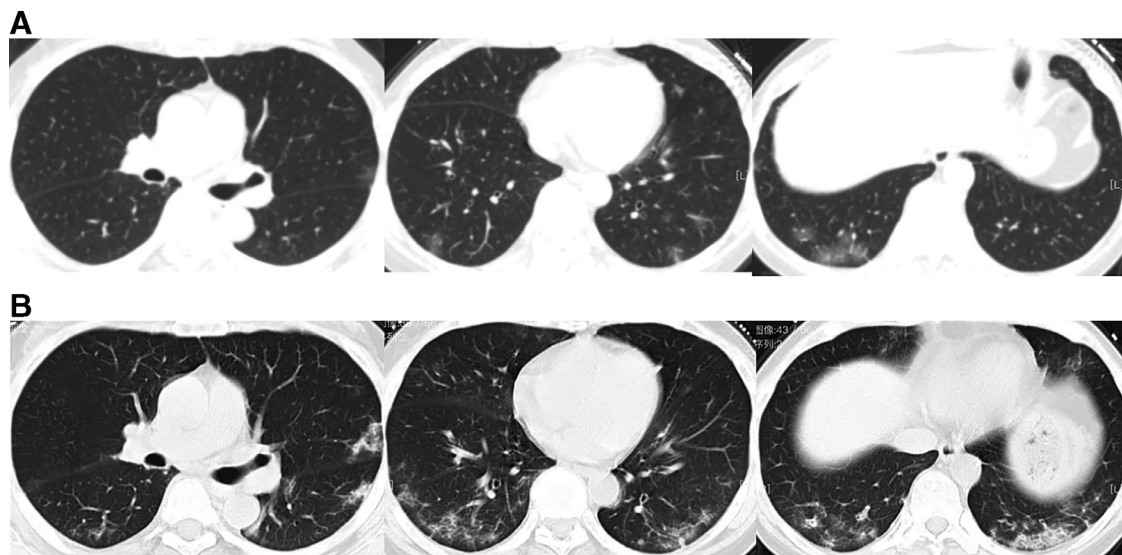


Fig. 7. A 66-year-old female patient with Coronavirus disease (COVID-19) pneumonia. (A) CT images obtained on day 4 after onset of the disease show scattered patchy ground glass opacities in both lungs, which are distributed peripherally. (B) CT images obtained on day 12 after the onset of the disease show the progression of the disease, with the number, range and densities of the lesions in both lungs increased.

lesions. Other findings included distortion of local lung structures, bronchodilation, and focal atelectasis.

In the severe phase of COVID-19, the pulmonary lesions generally reached peaked around 14 days after the onset of the disease, but a few cases developed rapidly, with the lesions appearing bilaterally with diffuse infiltration of all segments of the lungs, and manifesting as "white lung." Air bronchograms (Fig 8), suggested a large amount of cellular exudation in the alveolar cavity. Subsegmental atelectasis or reduction of lung volume was sometimes noted, and a small amount of pleural fluid could be seen bilaterally. The clinical symptoms were consistent with the severe type clinical manifestation. However, unlike SARS, occurrence of both pneumo-mediastinum and subcutaneous gas were rare (18,19).

The dissipative phase was seen most commonly after 14 days, and showed gradual absorption of the lesions, leaving

a few cord-like high-density shadows (Fig 9), indicative of fibrosis. In a few cases, the course of the disease was shorter, and the imaging manifestations progressed directly from the early stage into the dissipative phase.

CRITERIA FOR RELEASING FROM QUARANTINE AND DISCHARGE

The following criteria were used to guide release of patients from quarantine: patients were released if one or more of the following were present: (1) the body temperature returned to normal for more than 3 days. (2) respiratory symptoms improved significantly. (3) chest imaging showed significant improvement with reabsorption of acute exudative lesions. (4) the nucleic acid tests of samples from the respiratory tract were negative on two consecutive tests (the sampling time interval was at least one day).

APPLICATIONS OF AI IN THE PNEUMONIA OF COVID-19

During an epidemic such as is occurring with COVID-19 pneumonia, with an urgent need to diagnose and treat a large number of patients, artificial intelligence (AI) techniques can assist radiologists to identify the novel coronavirus pneumonia and accurately segment the areas of pneumonia, thus facilitating accurate and prompt assessment of the severity of the lesions (20) (Fig 10). Furthermore, since the COVID-19 pneumonia and other viral pneumonias have overlapping imaging manifestations, AI deep learning algorithms may prove beneficial in providing new insights for the differential diagnosis.

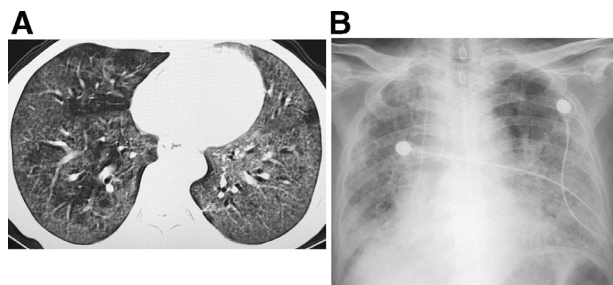


Fig. 8. A 68-year-old female patient with Coronavirus disease (COVID-19) pneumonia. (A) On day 11 from onset of the disease, the CT images show extensive ground-glass opacities and consolidations in both lungs. (B) On day 15 after onset of the disease, the condition deteriorate further, the chest radiography show extensive consolidations in both lungs, and the patient died on day 18.

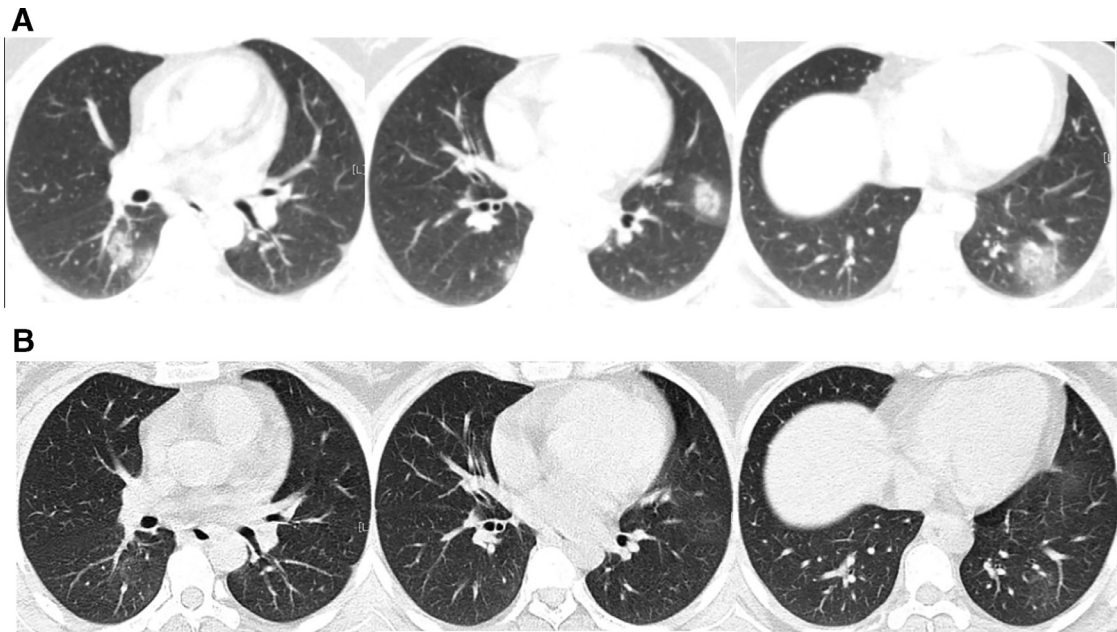


Fig. 9. A 35-year-old female patient with Coronavirus disease (COVID-19) pneumonia. (A) High-resolution CT scan obtained on day 4 from the onset of symptoms shows multiple nodular consolidations and ground glass opacities in both lungs, which are distributed along the bronchi bundles and the periphery of the lungs. (B) CT reexaminations on day 12 from onset of the disease show that most of the lung lesions have almost been absorbed.

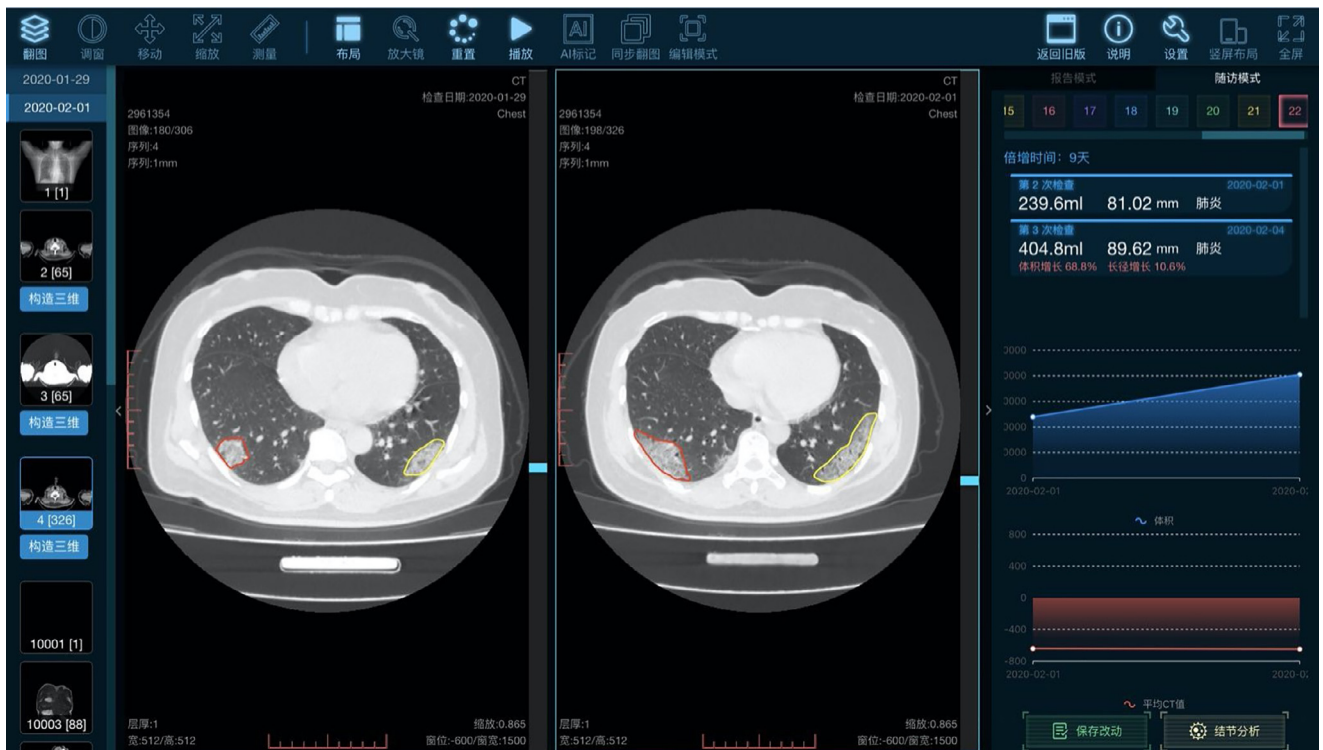


Fig. 10. Application of artificial intelligence (AI) in COVID-19. AI can accurately segment the lesion area and calculate the volume of the lesion, besides, it can also provide follow-up function for the cases, thus enabling the doctors to quickly compare the patient's conditions and evaluate the treatment efficacy.

CONCLUSION

CT plays an important role in the diagnosis, staging, and monitoring of patients with COVID-19 pneumonia. In the early phase, multiple small patchy shadows and interstitial changes emerge, and show a distribution starting near the pleura or bronchi rather than pulmonary parenchyma. In the progressive phase, the lesions increase and enlarge, developing into multiple GGOs as well as infiltrating consolidation in both lungs. In the severe phase, massive pulmonary consolidations and “white lungs” are seen, but pleural effusion is rare. In the dissipative phase, the GGOs and pulmonary consolidations were completely absorbed, and the lesions began to change into fibrosis.

REFERENCES

1. Li Q, Guan X, Wu P, et al. Early transmission dynamics in Wuhan, China, of novel coronavirus-infected pneumonia. *N Engl J Med* 2020. doi:10.1056/NEJMoa2001316.
2. Chen N, Zhou M, Dong X, et al. Epidemiological and clinical characteristics of 99 cases of 2019 novel coronavirus pneumonia in Wuhan, China: a descriptive study. *Lancet* 2020; 395(10223):507–513.
3. Wu F, Zhao S, Yu B, et al. A new coronavirus associated with human respiratory disease in China. *Nature* 2020. doi:10.1038/s41586-020-2008-3.
4. Zhu N, Zhang D, Wang W, et al. A novel coronavirus from patients with pneumonia in China, 2019. *N Engl J Med* 2020; 382(8):727–733.
5. Wrapp D, Wang N, Corbett KS, et al. Cryo-EM structure of the 2019-nCoV spike in the prefusion conformation. *Science* 2020. doi:10.1126/science.abb2507.
6. Zhang HW, Yu J, Xu HJ, et al. Corona virus international public health emergencies: implications for radiology management. *Acad Radiol* 2020. doi:10.1016/j.acra.2020.02.003.
7. Pan F, Ye T, Sun P, et al. Time course of lung changes on chest CT during recovery from 2019 novel coronavirus (COVID-19) pneumonia. *Radiology* 2020;200370. doi:10.1148/radiol.2020200370.
8. Fang Y, Zhang H, Xie J, et al. Sensitivity of chest CT for COVID-19: comparison to RT-PCR. *Radiology* 2020;200432. doi:10.1148/radiol.2020200432.
9. Liu P, Tan XZ. 2019 novel coronavirus (2019-nCoV) pneumonia. *Radiology* 2020;200257. doi:10.1148/radiol.2020200257.
10. Zu ZY, Jiang MD, Xu PP, et al. Coronavirus disease 2019 (COVID-19): a perspective from China. *Radiology* 2020;200490. doi:10.1148/radiol.2020200490.
11. Pan Y, Guan H, Zhou S, et al. Initial CT findings and temporal changes in patients with the novel coronavirus pneumonia (2019-nCoV): a study of 63 patients in Wuhan, China. *Eur Radiol* 2020. doi:10.1007/s00330-020-06731-x.
12. Kim JY, Ko JH, Kim Y, et al. Viral load kinetics of SARS-CoV-2 infection in first two patients in Korea. *J Korean Med Sci* 2020; 35(7):e86.
13. Lin X, Gong Z, Xiao Z, et al. Novel coronavirus pneumonia outbreak in 2019: computed tomographic findings in two cases. *Korean J Radiol* 2020. doi:10.3348/kjr.2020.0078.
14. Bernheim A, Mei X, Huang M, et al. Chest CT findings in coronavirus disease-19 (COVID-19): relationship to duration of infection. *Radiology* 2020;200463. doi:10.1148/radiol.2020200463.
15. Kanne JP. Chest CT findings in 2019 novel coronavirus (2019-nCoV) infections from Wuhan, China: key points for the radiologist. *Radiology* 2020;200241. doi:10.1148/radiol.2020200241.
16. Lei J, Li J, Li X, et al. CT Imaging of the 2019 novel coronavirus (2019-nCoV) pneumonia. *Radiology* 2020; 295(1):200236. doi:10.1148/radiol.2020200236.
17. Chung M, Bernheim A, Mei X, et al. CT imaging features of 2019 novel coronavirus (2019-nCoV). *Radiology* 2020;200230. doi:10.1148/radiol.2020200230.
18. Chan MS, Chan IY, Fung KH, Poon E, Yam LY, Lau KY. High-resolution CT findings in patients with severe acute respiratory syndrome: a pattern-based approach. *AJR Am J Roentgenol* 2004; 182:49–56.
19. Rao TN, Paul N, Chung T, et al. Value of CT in assessing probable severe acute respiratory syndrome. *AJR Am J Roentgenol* 2003; 181(2):317–319.
20. Long JB, Ehrenfeld JM. The role of augmented intelligence (AI) in detecting and preventing the spread of novel coronavirus. *J Med Syst* 2020; 44(3):59.